

Lyapunov exponents and geodesic stability of Schwarzschild black hole in the non-coomutative gauge theory of gravity

Abdellah Touati^{1,*} and Zaim Slimane^{1,†}

¹*Department of Physics, Faculty of Sciences of Matter, University of Batna-1, Batna 05000, Algeria*

(Dated: May 6, 2024)

In this paper, we study the stability of geodesic motion for both massive and massless particles using Lyapunov exponents in the non-commutative (NC) Schwarzschild black hole (SBH) via the gauge theory of gravity. As a first step, we investigate the both time-like and null radial motion of particles, the mean result in NC geometry shows that the particles take infinity proper time to reach the NC singularity (infinite time affine parameter framework for photons). The proper/coordinate time of Lyapunov exponents and their ratio of time-like geodesic for the circular motion of this black hole shows a new behavior, which describes a new range of stable circular orbits between unstable ones. Then we analyze the circular motion of photons, where the result shows a new photon sphere near the event horizon which is not allowed in the commutative case, and the Lyapunov exponent is expressed in this geometry, where this confirms the instability of the outer photon sphere and the stability of the inner one. Finally, we check the effect of the non-commutativity on the shadow radius of the SBH, where we show the similarity between the non-commutativity and the black hole mass.

I. INTRODUCTION

Studying the geodesic motion of a test body around a compact object has great importance in astrophysics to understand the physics of compact objects, such as neutron stars, black holes,..etc. The motion of particles around the black hole reveals a lot to understand their nature and geometrical propriety, such as the motion of stars around the galactic center for example the S-Sagittarius A* in the Milky Way galaxy [1–4]. There are two interesting kinds of geodesic motion in the study of black holes, which are radial and circular geodesic. There are many references that studied in detail the geodesic movement around black holes, such as [5–29]. Also, the classification of stable and unstable orbits is interesting to describe the geometrical proprieties of spacetime around compact objects. Among the various methods for analyzing the stability of geodesics, the Lyapunov exponent [30] has a great application in this context, in which this exponent is considered as a bridge between the non-linear general relativity and the non-linear dynamics. The Lyapunov exponent measures the average rate of separation between two nearby geodesics in phase space, in which the unstable geodesic can be expressed by the real Lyapunov exponent and the stable and marginal stable one are described by the imaginary and zero Lyapunov exponent respectively [31–41].

However, our interest is to investigate the geodesic stability via the Lyapunov exponent in NC spacetime. The NC theory is mainly motivated by string theory, being a limit in the presence of a background field [42–49]. The main idea results in the concept of quantifying spacetime leading to quantifying gravity, these quantum gravity effects can be neglected in low energy limits, but in the strong gravitational field of a black hole, one has to consider these effects. In the NC spacetime, the coordinate operators satisfy the following commutation relations:

$$[x^\mu, x^\nu] = i\Theta^{\mu\nu} \quad (1)$$

where $\Theta^{\mu\nu}$ is an anti-symmetric real matrix that determines the fundamental cell discretization of space-time. This commutation relation between coordinates themselves leads to the modification of Heisenberg uncertainty relations in such a way that prevents one from measuring positions with better accuracy than the Planck length.

$$\Delta\hat{x}^\mu\Delta\hat{x}^\nu \geq \frac{1}{2}|\Theta^{\mu\nu}| \quad (2)$$

In the NC theory, the ordinary product has changed to the star product (Moyal product) “*” between two arbitrary functions $f(x)$ and $g(x)$ defined over this space-time:

$$(f * g)(x) = f(x) e^{\frac{i}{2}\Theta^{\mu\nu}\overleftarrow{\partial}_\mu\overrightarrow{\partial}_\nu} g(x) \quad (3)$$

*Electronic address: touati.abph@gmail.com, abdellah.touati@univ-batna.dz

†Electronic address: zaim.abph@gmail.com

Recently there has been interest in studies that investigated the geodesic motion affected by the non-commutativity [50–62], and its stability using Lyapunov exponent [63–65]. Here one uses a gauge gravity theory in NC spacetime with star products and Seiberg-Witten (SW) map [66]. The NC gauge gravity is considered a theory beyond general relativity, which is an extended theory to the NC spacetime. In the NC gauge theory of gravity, the transformation of the action under the NC canonical transformations of NC fields via the SW map is invariant [67–69]. Our work will be in this context, to write the effective potential and Lyapunov exponent that arises from the deformed metric tensor which has been obtained using the star product between tetrads fields and the SW map. In addition, we hope to obtain corrections in terms of the NC parameter Θ for each of the effective potentials and the Lyapunov exponent and we also discussed the issue of the stability of circular orbits in the NC Schwarzschild geometry. The paper is organized as follows. In Sect. 2 we present the NC corrections to the metric field using star product and SW maps. In Sect. 3 we calculate the NC geodesic equation and we also obtain NC effective potentials up to the second-order in Θ . In Sect. 4 we investigate the radial and circular motion of massive and massless particles in this geometry, then we investigate the stability of orbits using the Lyapunov exponent. We then present the NC correction to the shadow radius of SBH. In the last section, we present our concluding remarks.

II. NON-COMMUTATIVE CORRECTIONS FOR SCHWARZSCHILD BLACK HOLE

In our previous works [62, 70], we used the tetrad formalism and both the star $*$ -product and the SW map to construct a non-commutative gauge theory for a static metric with a spherical symmetry. One can use a perturbation form for the SW map to describe the deformed tetrad fields $\hat{e}_\mu^a(x, \Theta)$ as a development in the power of Θ up to the second-order, which can be obtained by following the same approach in Ref. [71]:

$$\begin{aligned} \hat{e}_\mu^a = e_\mu^a - \frac{i}{4} \Theta^{\nu\rho} [\omega_\nu^{ac} \partial_\rho e_\mu^d + (\partial_\rho \omega_\mu^{ac} + R_{\rho\mu}^{ac}) e_\nu^d] \eta_{cd} \\ + \frac{1}{32} \Theta^{\nu\rho} \Theta^{\lambda\tau} \left[2\{R_{\tau\nu}, R_{\mu\rho}\}^{ab} e_\lambda^c - \omega_\lambda^{ab} (D_\rho R_{\tau\nu}^{cd} + \partial_\rho R_{\tau\nu}^{cd}) e_\nu^m \eta_{dm} \right. \\ - \{\omega_\nu, (D_\rho R_{\tau\nu} + \partial_\rho R_{\tau\nu})\}^{ab} e_\lambda^c - \partial_\tau \{\omega_\nu, (\partial_\rho \omega_\mu + R_{\rho\mu})\}^{ab} e_\lambda^c \\ - \omega_\lambda^{ab} (\omega_\nu^{cd} \partial_\rho e_\mu^m + (\partial_\rho \omega_\mu^{cd} + R_{\rho\mu}^{cd}) e_\nu^m) \eta_{dm} + 2\partial_\nu \omega_\lambda^{ab} \partial_\rho \partial_\tau e_\lambda^c \\ - 2\partial_\rho (\partial_\tau \omega_\mu^{ab} + R_{\tau\mu}^{ab}) \partial_\nu e_\lambda^c - \{\omega_\nu, (\partial_\rho \omega_\lambda + R_{\rho\lambda})\}^{ab} \partial_\tau e_\mu^c \\ \left. - (\partial_\tau \omega_\mu + R_{\tau\mu}) (\omega_\nu^{cd} \partial_\rho e_\lambda^m + ((\partial_\rho \omega_\lambda + R_{\rho\lambda})) e_\nu^m) \eta_{dm} \right] \eta_{cb} + \mathcal{O}(\Theta^3), \end{aligned} \quad (4)$$

where \hat{e}_a^μ and ω_μ^{ab} are the tetrad field and the spin connection (gauge field), and:

$$\{\alpha, \beta\}^{ab} = (\alpha^{ac} \beta^{db} + \beta^{ac} \alpha^{db}) \eta_{cd}, \quad [\alpha, \beta]^{ab} = (\alpha^{ac} \beta^{db} - \beta^{ac} \alpha^{db}) \eta_{cd} \quad (5)$$

$$D_\mu R_{\rho\sigma}^{ab} = \partial_\mu R_{\rho\sigma}^{ab} + (\omega_\mu^{ac} R_{\rho\sigma}^{db} + \omega_\mu^{bc} R_{\rho\sigma}^{da}) \quad (6)$$

where the \hat{e}_a^μ is the of the vierbein \hat{e}_μ^a defined as:

$$\hat{e}_\mu^b \hat{e}_a^\mu = \delta_a^b, \quad \hat{e}_\mu^a \hat{e}_a^\nu = \delta_\mu^\nu. \quad (7)$$

In the following, we consider a symmetric metric $\hat{g}_{\mu\nu}$, so that:

$$\hat{g}_{\mu\nu} = \frac{1}{2} (\hat{e}_\mu^b * \hat{e}_{\nu b} + \hat{e}_\nu^b * \hat{e}_{\mu b}). \quad (8)$$

To compute the deformed metric $\hat{g}_{\mu\nu}$, we choose the following NC anti-symmetric matrix $\Theta^{\mu\nu}$:

$$\Theta^{\mu\nu} = \begin{pmatrix} 0 & 0 & 0 & 0 \\ 0 & 0 & 0 & \Theta \\ 0 & 0 & 0 & 0 \\ 0 & -\Theta & 0 & 0 \end{pmatrix}, \quad \mu, \nu = 0, 1, 2, 3 \quad (9)$$

We follow the same steps outlined in Ref. [62], we choose the following general tetrads field:

$$e_\mu^0 = \left(\left(1 - \frac{2m}{r}\right)^{\frac{1}{2}}, 0, 0, 0 \right), \quad (10)$$

$$\underline{e}_\mu^1 = \begin{pmatrix} 0 & \left(1 - \frac{2m}{r}\right)^{-\frac{1}{2}} \sin\theta \cos\phi & r \cos\theta \cos\phi & -r \sin\theta \sin\phi \end{pmatrix}, \quad (11)$$

$$\underline{e}_\mu^2 = \begin{pmatrix} 0 & \left(1 - \frac{2m}{r}\right)^{-\frac{1}{2}} \sin\theta \sin\phi & r \cos\theta \sin\phi & r \sin\theta \cos\phi \end{pmatrix}, \quad (12)$$

$$\underline{e}_\mu^3 = \begin{pmatrix} 0 & \left(1 - \frac{2m}{r}\right)^{-\frac{1}{2}} \cos\theta & -r \sin\theta & 0 \end{pmatrix}. \quad (13)$$

The non-zero components of the NC tetrad fields \hat{e}_μ^a are calculated in Ref. [62]. Then, using the definition (8), we obtain the following non-zero components of the non-commutative metric $\hat{g}_{\mu\nu}$ up to second order of Θ , we take the case $\theta = \pi/2$:

$$-\hat{g}_{tt} = \left(1 - \frac{2m}{r}\right) + \left\{ \frac{m \left(88m^2 + mr \left(-77 + 15\sqrt{1 - \frac{2m}{r}} \right) - 8r^2 \left(-2 + \sqrt{1 - \frac{2m}{r}} \right) \right)}{16r^4(-2m+r)} \right\} \Theta^2 + \mathcal{O}(\Theta^4) \quad (14)$$

$$\hat{g}_{rr} = \left(1 - \frac{2m}{r}\right)^{-1} + \left\{ \frac{m \left(12m^2 + mr \left(-14 + \sqrt{1 - \frac{2m}{r}} \right) - r^2 \left(5 + \sqrt{1 - \frac{2m}{r}} \right) \right)}{8r^2(2m-r)^3} \right\} \Theta^2 + \mathcal{O}(\Theta^4) \quad (15)$$

$$\hat{g}_{\theta\theta} = r^2 + \left\{ \frac{m \left(m \left(10 - 6\sqrt{1 - \frac{2m}{r}} \right) - \frac{8m^2}{r} + r \left(-3 + 5\sqrt{1 - \frac{2m}{r}} \right) \right)}{16(-2m+r)^2} \right\} \Theta^2 + \mathcal{O}(\Theta^4) \quad (16)$$

$$\hat{g}_{\phi\phi} = r^2 + \left\{ \frac{5}{8} - \frac{3}{8}\sqrt{1 - \frac{2m}{r}} + \frac{m \left(-17 + \frac{5}{\sqrt{1 - \frac{2m}{r}}} \right)}{16r} + \frac{m^2 \sqrt{1 - \frac{2m}{r}}}{(-2m+r)^2} \right\} \Theta^2 + \mathcal{O}(\Theta^4) \quad (17)$$

It is clear that, for $\Theta \rightarrow 0$, we obtain the commutative Schwarzschild solution. For such a black hole, we find that the static limit surface and the event horizon in the non-commutative spacetime is where the NC metric (14)-(15) satisfies the following conditions:

$$\hat{g}_{00} = 0, \quad 1/\hat{g}_{rr} = 0. \quad (18)$$

The solution to this equations gives us respectively the NC static limit surface and the event horizon of the SBH [62, 70]:

$$r_{sls}^{NC} = r_h \left[1 + \left(\frac{\Theta}{r_h} \right) \left(\frac{4\sqrt{5}+1}{32\sqrt{5}} \right) + \left(\frac{\Theta}{r_h} \right)^2 \left(\frac{10+\sqrt{5}}{128} \right) \right], \quad (19)$$

and

$$r_h^{NC} = r_h \left[1 + \frac{3}{8} \left(\frac{\Theta}{r_h} \right)^2 \right]. \quad (20)$$

where $r_h = 2m$ is the event horizon in commutative case when $\Theta = 0$. The effect of non-commutativity is small, which is reasonable to expect since at large distances it can be neglected.

III. GEODETIC MOTION AND ITS STABILITY AROUND A NON-RECIPROCAL SCHWARZSCHILD BLACK HOLE

In this section we investigate the stability of circular orbit in the equatorial plane (i.e. $\theta = \frac{\pi}{2}$) in the deformed Schwarzschild background, which is given by the following line element

$$d\hat{s}^2 = \hat{g}_{tt}(r, \Theta) c^2 dt^2 + \hat{g}_{rr}(r, \Theta) dr^2 + \hat{g}_{\phi\phi}(r, \Theta) d\phi^2 \quad (21)$$

According to the above deformed line element, the Lagrangian for test particles motion in NC spacetime is given by

$$2\mathcal{L} = \hat{g}_{tt}(r, \Theta)c^2\dot{t}^2 + \hat{g}_{rr}(r, \Theta)\dot{r}^2 + \hat{g}_{\phi\phi}(r, \Theta)\dot{\phi}^2 \quad (22)$$

where the dot refers to the differentiation with respect to the affine parameter τ .

Using the Euler-Lagrange equation to compute the generalized momenta:

$$p_t = c^2\hat{g}_{tt}(r, \Theta)\dot{t} = E_0 = \text{const}, \quad (23)$$

$$p_\phi = \hat{g}_{\phi\phi}(r, \Theta)\dot{\phi} = l = \text{const}, \quad (24)$$

$$p_r = \hat{g}_{rr}(r, \Theta)\dot{r} \quad (25)$$

The Lagrangian \mathcal{L} is independent of t and ϕ so we have two conserved quantities p_t (energy E_0) and p_ϕ (angular momentum l), and that gives us:

$$\dot{t} = \frac{E_0}{c^2\hat{g}_{tt}(r, \Theta)}, \quad \dot{\phi} = \frac{l}{\hat{g}_{\phi\phi}(r, \Theta)}. \quad (26)$$

Substitute these two quantities into the invariant¹ of $\hat{g}_{\mu\nu}U^\mu U^\nu \equiv -h$, after some algebra we get the explicit equation for \dot{r}^2 :

$$\dot{r}^2 = -\frac{E_0^2}{c^2\hat{g}_{tt}(r, \Theta)\hat{g}_{rr}(r, \Theta)} - \frac{1}{\hat{g}_{rr}(r, \Theta)} \left(\frac{l^2}{\hat{g}_{\phi\phi}(r, \Theta)} + hc^2 \right) \quad (27)$$

where we shall consider $h = 1$ for massive particles and $h = 0$ for massless ones.

Substituting Eqs. (14), (15) and (17) into (27), we find the :

$$\dot{r}^2 + V_{eff}(r, \Theta) = 0 \quad (28)$$

where $V_{eff}(r, \Theta)$ represents the deformed effective potential, and it is developed up to the second order in Θ , which reads:

$$\begin{aligned} V_{eff}(r, \Theta) = & \left(1 - \frac{2m}{r}\right) \left(\frac{l^2}{r^2} + hc^2\right) - E^2 + \Theta^2 \left\{ -\frac{l^2}{r^4} \left(1 - \frac{2m}{r}\right) \left(\frac{5}{8} - \frac{3}{8}\sqrt{1 - \frac{2m}{r}} + \frac{m \left(-17 + \frac{5}{\sqrt{1 - \frac{2m}{r}}}\right)}{16r} \right. \right. \\ & + \frac{m^2 \sqrt{1 - \frac{2m}{r}}}{(-2m + r)^2} \Bigg) + E^2 \left(\frac{m(64m^2 + m(-49 + 13\sqrt{1 - \frac{2m}{r}})r + 2(13 - 3\sqrt{1 - \frac{2m}{r}})r^2)}{16r^5(1 - \frac{2m}{r})^2} \right) \\ & \left. + \left(\frac{l^2}{r^2} + hc^2\right) \left(\frac{m(12m^2 + m(-14 + \sqrt{1 - \frac{2m}{r}})r - (5 + \sqrt{1 - \frac{2m}{r}})r^2)}{8r^5(1 - \frac{2m}{r})} \right) \right\} + \mathcal{O}(\Theta^4) \end{aligned} \quad (29)$$

It is clear, for $\Theta \rightarrow 0$, we obtain the commutative effective potential for the Schwarzschild metric:

$$V_{eff}(r, \Theta = 0) = \left(1 - \frac{2m}{r}\right) \left(\frac{l^2}{r^2} + hc^2\right) - E^2. \quad (30)$$

A. Radial motion of massive particles

To investigate the radial motion of massive particle in the NC SBH spacetime we must use the above effective potential (29) with $l = 0$ and $h = 1$, $c = 1$, which give us the effective potential for a radial motion of massive

¹ where $U^\mu = c^{-1} \frac{dx^\mu}{d\tau}$ denotes the 4-velocity.

particle in NC spacetime

$$\left(\frac{dr}{d\tau}\right)^2 = E^2 - \left(1 - \frac{2m}{r}\right) - \Theta^2 \left\{ E^2 \left(\frac{m(64m^2 + m(-49 + 13\sqrt{1 - \frac{2m}{r}})r + 2(13 - 3\sqrt{1 - \frac{2m}{r}})r^2)}{16r^5(1 - \frac{2m}{r})^2} \right) + \left(\frac{m(12m^2 + m(-14 + \sqrt{1 - \frac{2m}{r}})r - (5 + \sqrt{1 - \frac{2m}{r}})r^2)}{8r^5(1 - \frac{2m}{r})} \right) \right\} + \mathcal{O}(\Theta^4) \quad (31)$$

It is clear that the above equation (31) reduces the commutative radial equation of massive particle in SBH when $\Theta = 0$. Let's consider now a free fall of massive particle in the NC SBH, which is initially at rest i.e., $\dot{r} = 0$ and located at $r = r_0$ when $\tau = 0$. The proper time in NC spacetime can be defined using the above equation (31) with $E = 1$

$$\hat{\tau} = - \int_{r_0}^r \left(\frac{2m}{r'} - \Theta^2 \left\{ \left(\frac{m(64m^2 + m(-49 + 13\sqrt{1 - \frac{2m}{r'}})r' + 2(13 - 3\sqrt{1 - \frac{2m}{r'}})r'^2)}{16r'^5(1 - \frac{2m}{r'})^2} \right) + \left(\frac{m(12m^2 + m(-14 + \sqrt{1 - \frac{2m}{r'}})r' - (5 + \sqrt{1 - \frac{2m}{r'}})r'^2)}{8r'^5(1 - \frac{2m}{r'})} \right) \right\} \right)^{-1/2} dr', \quad (32)$$

the proper time at the leading order of Θ , is given by :

$$\begin{aligned} \hat{\tau} = & \frac{2}{3} \left(\sqrt{\frac{r_0^3}{2m}} - \sqrt{\frac{r^3}{2m}} \right) + \Theta^2 \left\{ \sqrt{\frac{r_0}{2m}} \left(\frac{32m^2 + 4m(-52 + \sqrt{1 - \frac{2m}{r_0}})r_0 + 131r_0^2}{128(2m - r_0)r_0^2} \right) \right. \\ & - \sqrt{\frac{r}{2m}} \left(\frac{32m^2 + 4m(-52 + \sqrt{1 - \frac{2m}{r}})r + 131r^2}{128(2m - r)r^2} \right) + \frac{1}{8m} \left(\text{ArcSin} \left(\sqrt{\frac{2m}{r_0}} \right) - \text{ArcSin} \left(\sqrt{\frac{2m}{r}} \right) \right) \\ & \left. + \frac{67}{256m} \left(\text{ArcTanh} \left(\sqrt{\frac{r_0}{2m}} \right) - \text{ArcTanh} \left(\sqrt{\frac{r}{2m}} \right) \right) \right\}. \end{aligned} \quad (33)$$

the commutative expression of proper time can be obtained by setting $\Theta = 0$.

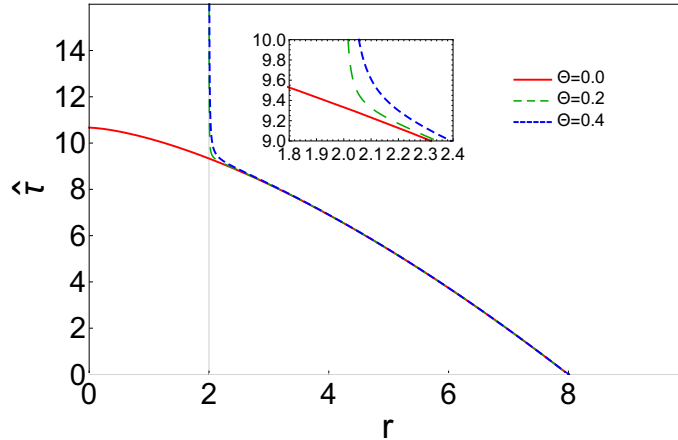


FIG. 1 The behavior of the proper time of free fall for massive particle in the NC SBH as a function of r , with $m = 1$ and the initial position $r_0 = 8$.

Fig. 1 shows the behavior of proper time $\hat{\tau}$ for a free fall of a massive particle into NC SBH. As we observe, the effect of the non-commutativity on the proper time is located near the event horizon, where its effect is to increase the proper time of a massive particle near the event horizon with the increase of Θ , and in this geometry, the massive

particles take an infinite time to reach the NC singularity (see Ref. [62]) contrary to the commutative behavior [5], and this effect disappears when we move away from the event horizon.

The coordinate time for the free fall in the NC SBH can be obtained using the relation (26) with (31) and setting $E = 1$, we get:

$$\hat{t} = - \int_{r_0}^r (\hat{g}_{tt})^{-1} \left(\frac{2m}{r'} - \Theta^2 \left\{ \left(\frac{m(64m^2 + m(-49 + 13\sqrt{1 - \frac{2m}{r'}})r' + 2(13 - 3\sqrt{1 - \frac{2m}{r'}})r'^2)}{16r'^5(1 - \frac{2m}{r'})^2} \right) + \left(\frac{m(12m^2 + m(-14 + \sqrt{1 - \frac{2m}{r'}})r' - (5 + \sqrt{1 - \frac{2m}{r'}})r'^2)}{8r'^5(1 - \frac{2m}{r'})} \right) \right\} \right)^{-1/2} dr', \quad (34)$$

the above integral can be evaluated at the leading order in Θ ,

$$\begin{aligned} \hat{t} = & \frac{2}{3} \left(\sqrt{\frac{r_0^3}{2m}} - \sqrt{\frac{r^3}{2m}} \right) + 4m \left(\sqrt{\frac{r_0}{2m}} - \sqrt{\frac{r}{2m}} \right) - 4m \left(\text{ArcTanh} \left(\sqrt{\frac{r_0}{2m}} \right) - \text{ArcTanh} \left(\sqrt{\frac{r}{2m}} \right) \right) \\ & + \Theta^2 \left\{ \sqrt{\frac{r_0}{2m}} \left(-\frac{25}{16r_0} - \frac{37m}{128(r_0 - 2m)^2} + \frac{15\sqrt{1 - \frac{2m}{r_0}}}{32(r_0 - 2m)^2} - \frac{r_0\sqrt{1 - \frac{2m}{r_0}}}{4(r_0 - 2m)^2} - \frac{61}{512(r_0 - 2m)} \right) \right. \\ & - \sqrt{\frac{r}{2m}} \left(-\frac{25}{16r} - \frac{37m}{128(r - 2m)^2} + \frac{15\sqrt{1 - \frac{2m}{r}}}{32(r - 2m)^2} - \frac{r\sqrt{1 - \frac{2m}{r}}}{4(r - 2m)^2} - \frac{61}{512(r - 2m)} \right) \\ & \left. + \frac{1}{4m} \left(\text{ArcSin} \left(\sqrt{\frac{2m}{r_0}} \right) - \text{ArcSin} \left(\sqrt{\frac{2m}{r}} \right) \right) + \frac{605}{1024m} \left(\text{ArcTanh} \left(\sqrt{\frac{r_0}{2m}} \right) - \text{ArcTanh} \left(\sqrt{\frac{r}{2m}} \right) \right) \right\}. \quad (35) \end{aligned}$$

the commutative expression of time coordinate can be obtained by setting $\Theta = 0$.

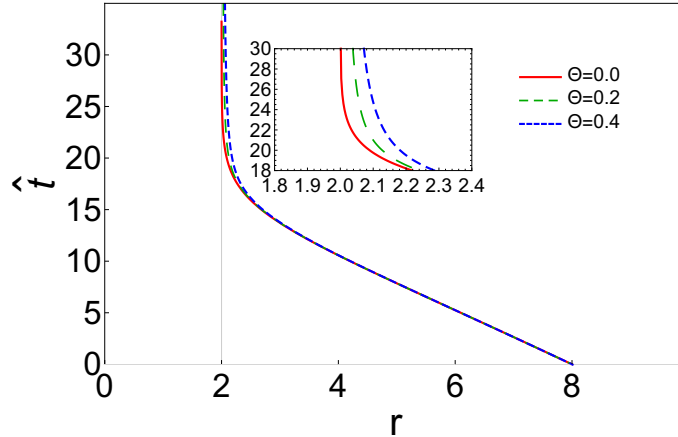


FIG. 2 The behavior of the time coordinate for a free fall of a massive particle in the NC SBH as a function of r , with $m = 1$ and the initial position $r_0 = 8$.

In Fig. 2 we show the behavior of the coordinate time \hat{t} for a free fall of a massive particle in the NC SBH. As we see, the effect of the non-commutativity on the time coordinate is located near the NC event horizon, which is increasing the time coordinate of a massive particle near the NC event horizon compared to the commutative one, and that is a similar behavior to the commutative one [5].

Fig. 3 shows the variation of the proper time and coordinate time of massive particle falling toward the NC SBH. The massive particles located at r_0 falling toward the NC SBH take an infinite time with both its own proper time and in the coordinate time to reach the NC singularity and the NC event horizon respectively, which is contrary to the commutative case for the proper time [5]. In this case, the non-commutativity prevents the massive test particles to reach the NC singularity at a finite time.

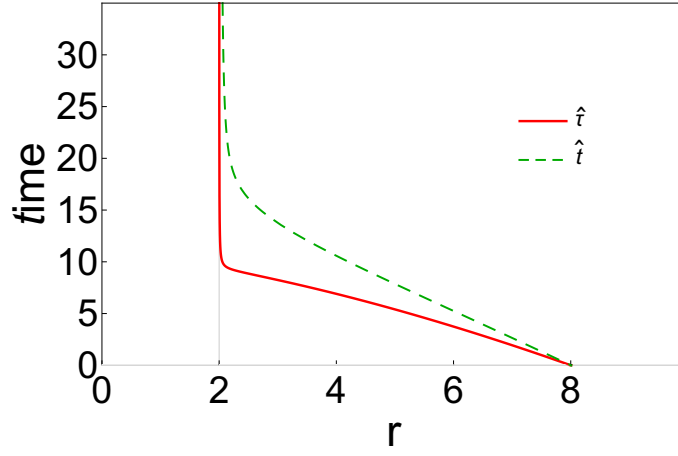


FIG. 3 The behavior of the proper/coordinate time of free fall for massive particle in the NC SBH as function of r , with $m = 1$ and the initial position $r_0 = 8$.

B. Circular motion of massive particles and Lyapunov exponents

The effective potential for a massive test particle is given by (29) with $h = 1, c = 1$, which is analyzed in detail in Ref. [62].

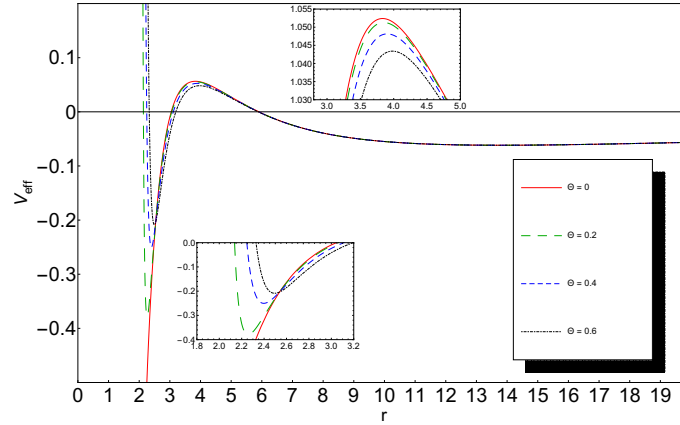


FIG. 4 The behavior of the energy E_c^2 (left panel) and angular momentum L_c^2 (right panel) of a circular orbit for a massive test particle in NC Schwarzschild spacetime.

The influence of the NC parameters Θ on the effective potential for a massive particle is shown in Fig. 4. As we see now a new minimum to the effective potential appears near the event horizon (whatever the values of angular momentum $l \geq 0$), where all the extremum of this potential are located outside the event horizon, which allows us to interpret this new minimum as a new stable circular orbit [62], which gives us multiple stable circular orbits in this geometry. It is worth noting that, the new minimum of the effective potential shifted away from the event horizon as Θ increases. As we can see, the NC effects become insignificant as we move further from the event horizon ($r \gg r_h^{NC}$).

Our aim now is to investigate the geodesic stability of the circular orbits for a massive particles. For this kind of motion, the effective potential must satisfy two conditions, which reads:

$$V_{eff}(r, \Theta) = 0, \frac{dV_{eff}}{dr} = 0. \quad (36)$$

using this two conditions, we can compute the energy and the angular momentum of massive particle for circular orbits:

$$E_c^2 \simeq \frac{(-2m + r_c)^2}{r_c(r_c - 3m)} - \left(\frac{B(r_c) + F(r_c)\sqrt{1 - \frac{2m}{r_c}}}{32(r_c^4(-3m + r_c)^2\sqrt{1 - \frac{2m}{r_c}})} \right) \Theta^2 + \mathcal{O}(\Theta^4), \quad (37)$$

$$L_c^2 \simeq \frac{mr_c^2}{r_c - 3m} - \left(\frac{S(r_c) + Q(r_c)\sqrt{1 - \frac{2m}{r_c}}}{32(r_c(-3m + r_c)^2(r_c - 2m)\sqrt{1 - \frac{2m}{r_c}})} \right) \Theta^2 + \mathcal{O}(\Theta^4). \quad (38)$$

where:

$$B(r_c) = -120m^4 + 162m^3r_c - 71m^2r_c^2 + 4mr_c^3, \quad F(r_c) = 204m^4 - 174m^3r_c + 41m^2r_c^2 - 4mr_c^3, \quad (39)$$

$$S(r_c) = -48m^4 + 126m^3r_c - 55m^2r_c^2, \quad Q(r_c) = -120m^4 + 174m^3r_c - 75m^2r_c^2 + 8mr_c^3. \quad (40)$$

in the limit of $\Theta \rightarrow 0$ we recover the commutative energy and angular momentum of the commutative SBH.

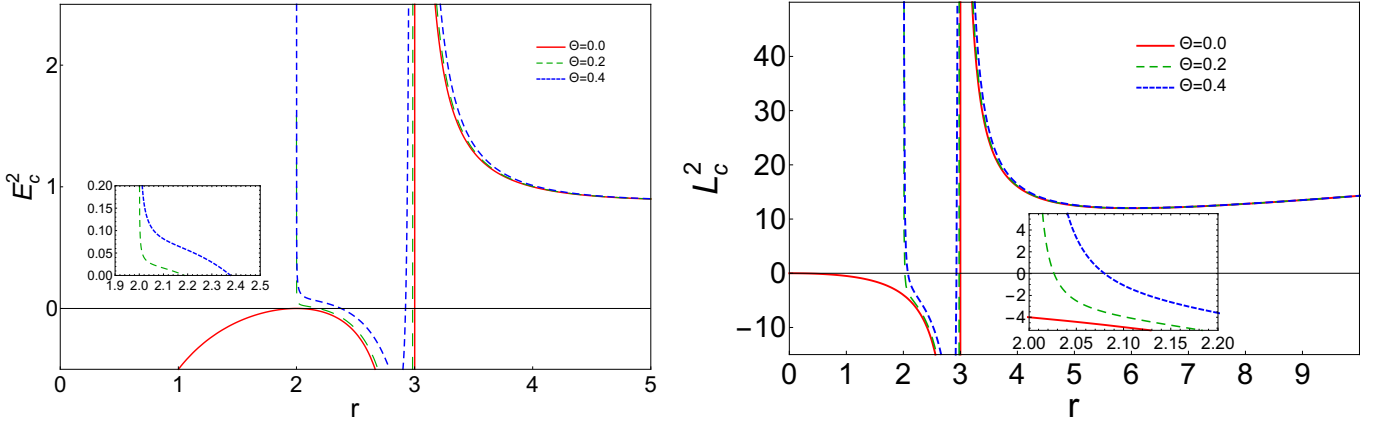


FIG. 5 The behavior of the effective potential for massive particle with different values of NC parameters Θ and fixed: $E = 0.998$, $m = 1$, $l = 4.2$.

Fig. 5 shows the behaviors of the angular momentum L_c^2 and energy E_c^2 of circular orbit for massive particles around NC SBH as a function of r_c . As we see the NC effect on the energy condition of circular orbit produces a new behavior above which the result becomes unphysical ($E_c^2 < 0$) (see the left panel) and it's turned to the positive values ($E_c^2 > 0$) near the event horizon, which is explained by the new ISCO at this region in the NC geometry. The NC effect on the angular momentum is shown in the right panel, and a new behavior is observed, as the observation in the energy, the angular momentum also has positive values near the event horizon which corresponds to the new stable circular orbit [62], Where in the commutative case $\Theta = 0$, the new behavior of energy and angular momentum disappears.

1. Time period and orbital velocity

The orbital velocity for a massive particle in NC Schwarzschild spacetime is given by [33, 65]

$$\hat{\Omega}_c = \frac{\dot{\phi}}{\dot{t}}, \quad (41)$$

using the Eq. (26) together with (37) and (38), the orbital velocity at the second order in the NC parameter Θ is

$$\hat{\Omega}_c = \sqrt{\frac{m}{r_c^3} + \left(\frac{X(r_c) + W(r_c)\sqrt{1 - \frac{2m}{r_c}}}{32r_c^6(r_c - 2m)^3} \right) \Theta^2}, \quad (42)$$

where

$$X(r_c) = -1272m^5 + 2304m^4r_c - 1544m^3r_c^2 + 451m^2r_c^3 - 48mr_c^4, \quad (43)$$

$$W(r_c) = -192m^4r_c + 298m^3r_c^2 - 137m^2r_c^3 + 24mr_c^4. \quad (44)$$

when $\Theta = 0$, we get the commutative case [33].

The orbital time scale (time period) of the coordinate time in NC spacetime is given by [33]

$$\hat{T}_{\Omega} = \frac{2\pi}{\hat{\Omega}_c}, \quad (45)$$

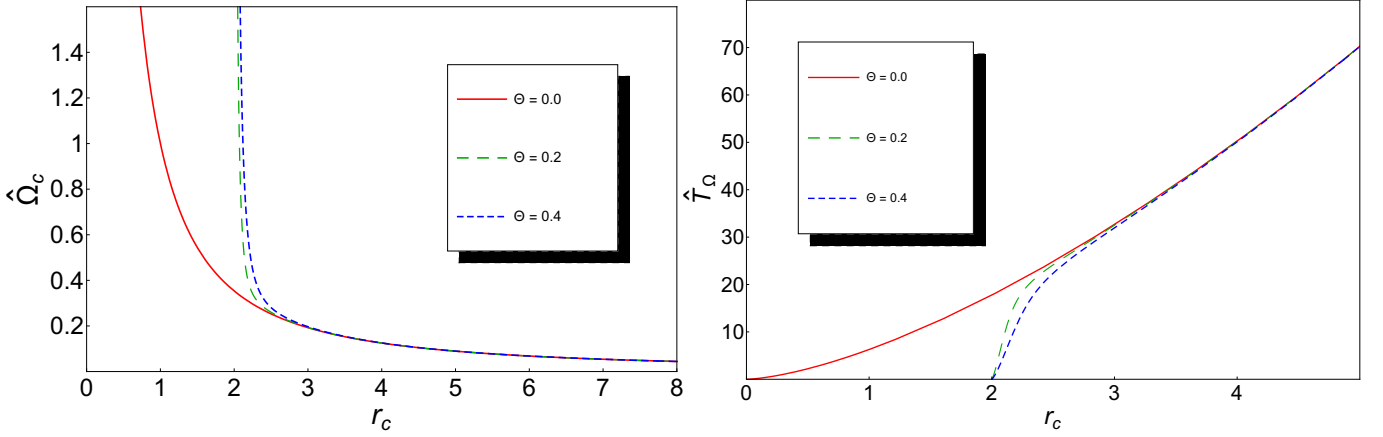


FIG. 6 The behavior of the NC orbital velocity (left panel) and NC orbital time scale (right panel) for a massive test particle.

In Fig. 6, we show the behavior of the orbital velocity (left panel) and orbital time scale of coordinate time (right panel) in the NC spacetime as a function of r_c . As we see the effect of the non-commutativity shows a new behavior in both orbital velocity (left panel) and orbital time scale (right panel), where the new behavior appears only outside the event horizon r_h^{NC} , where the non-commutativity increases the orbital velocity of a massive particle near the event horizon and at large orbit is negligible. The orbital time scale in the presence of the non-commutativity is smaller compared to the commutative case, and as we see the orbital time scale is zero at the event horizon, where the non-commutativity decreases the orbital time scale near the event horizon r_h^{NC} and at the large orbits $r_c \gg 3$ this effect vanish.

2. Lyapunov exponents

In order to analyze the stability and instability of circular geodesics of a massive test particle around the NC Schwarzschild black hole we use the Lyapunov exponents $\hat{\lambda}$, where that is determined by checking the nature of $\hat{\lambda}$. The circular orbit is stable when $\hat{\lambda}_p$ (or $\hat{\lambda}_c$) is imaginary and is unstable for $\hat{\lambda}_p$ (or $\hat{\lambda}_c$) real [37, 40]. The proper time Lyapunov exponents $\hat{\lambda}_p$ and coordinate time Lyapunov exponents $\hat{\lambda}_c$ in NC spacetime are given respectively by [33, 37, 39, 40]

$$\hat{\lambda}_p = \pm \sqrt{\frac{-V_{eff}(r, \Theta)''}{2}}, \quad \hat{\lambda}_c = \pm \sqrt{\frac{-V_{eff}(r, \Theta)''}{2\dot{t}^2}}. \quad (46)$$

using the effective potential (29) for massive particle together with (26), (37) and (38) we find

$$\hat{\lambda}_p = \sqrt{-\frac{m(r_c - 6m)}{(r_c - 3m)r_c^3} + \left(\frac{Z(r_c) + P(r_c)\sqrt{1 - \frac{2m}{r_c}}}{32(r_c - 2m)^3 r_c^6 (r_c - 3m)^2} \right) \Theta^2}, \quad (47)$$

$$\hat{\lambda}_c = \sqrt{-\frac{m(r_c - 6m)}{r_c^4} + \left(\frac{Y(r_c) + N(r_c)\sqrt{1 - \frac{2m}{r_c}}}{32(r_c - 2m)^3 r_c^7} \right) \Theta^2}. \quad (48)$$

where

$$Z(r_c) = 16416m^7 - 38544m^6 r_c + 34992m^5 r_c^2 - 16116m^4 r_c^3 + 4076m^3 r_c^4 - 551m^2 r_c^5 + 32mr_c^6, \quad (49)$$

$$P(r_c) = 3564m^6 r_c - 8058m^5 r_c^2 + 7070m^4 r_c^3 - 2910m^3 r_c^4 + 517m^2 r_c^5 - 24mr_c^6, \quad (50)$$

$$Y(r_c) = 8880m^6 - 16568m^5 r_c + 11200m^4 r_c^2 - 3470m^3 r_c^3 + 515m^2 r_c^4 - 32mr_c^5, \quad (51)$$

$$N(r_c) = 1668m^5 r_c - 2870m^4 r_c^2 + 1808m^3 r_c^3 - 473m^2 r_c^4 + 24mr_c^5, \quad (52)$$

the commutative expressions of $\hat{\lambda}_p$ and $\hat{\lambda}_c$ are recovered when $\Theta = 0$ [37, 39].

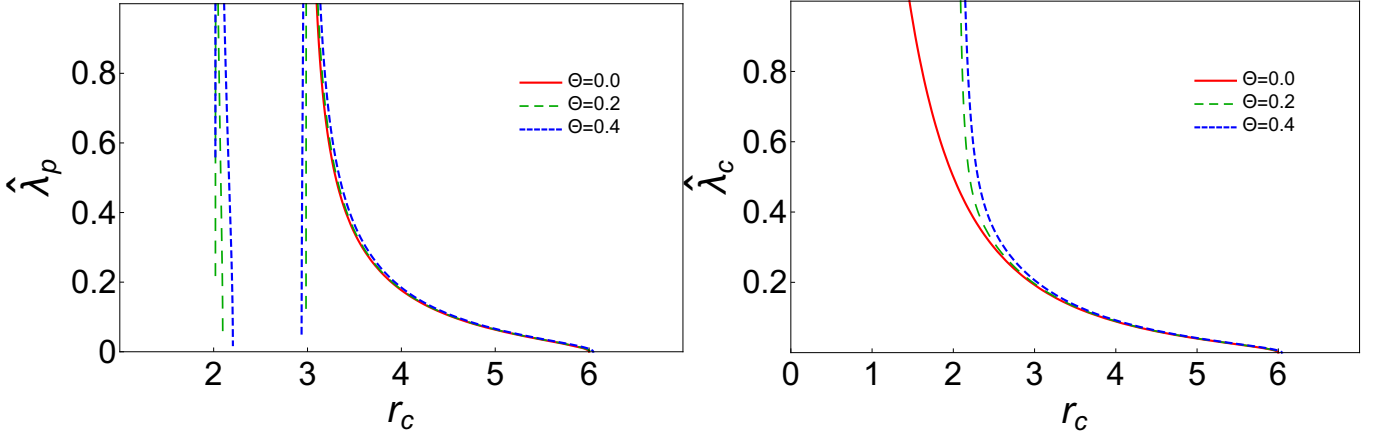


FIG. 7 The behavior of the proper time (left panel) and coordinate time (right panel) Lyapunov exponents for massive particle as function of circular orbits r_c .

The proper time and coordinate time of Lyapunov exponents in the NC spacetime for massive particles is shown in Fig. 7 (left and right panel respectively), which describes the instability of orbits. As we observe, in the NC spacetime a new behavior appears for both $\hat{\lambda}_p$ (left panel) and $\hat{\lambda}_c$ (right panel). The coordinate time Lyapunov exponents in the NC space time (right panel) shows the instability of the orbits in the region between the event horizon r_h^{NC} and the NC innermost stable circular orbit (ISCO) r_{outer}^{ISCO} , which means that $\hat{\lambda}_c$ is real in the region $r_h^{NC} < r_c \leq r_{outer}^{ISCO}$, and that means the orbits in this region are unstable, where the non-commutativity increases the instability of the orbits near the event horizon and its decreases with increase in the radius of circular orbit r_c , until reaching zero at the outer ISCO r_{outer}^{ISCO} . Moreover, the proper time Lyapunov exponents in the NC spacetime (left panel) show a different behavior to the coordinate time case for the instability of the circular orbit of a massive particle, where $\hat{\lambda}_p$ is real in two regions $r_h^{NC} < r_c \leq r_{inner}^{ISCO}$ and $r_c^{uns} < r_c \leq r_{outer}^{ISCO}$ which mean that the orbit of the particle is unstable and is imaginary in the region $r_{inner}^{ISCO} \leq r_c \leq r_c^{uns}$ and that means the circular orbit is stable, this result coincides with our previous work [62], where the new circular orbit near the event horizon is stable.

Now we compute ratio proper/coordinate time Lyapunov exponent is given by

$$\frac{\hat{\lambda}_p}{\hat{\lambda}_c} = \sqrt{\frac{r_c}{(r_c - 3m)} + \left(\frac{Y(r_c)(3m - r_c) - Z(r_c) + (N(r_c)(3m - r_c) - P(r_c))\sqrt{1 - \frac{2m}{r_c}}}{32m(r_c - 2m)^3(r_c - 3m)^2(r_c - 6m)r_c^2} \right) \Theta^2}, \quad (53)$$

in the case of $\Theta = 0$ the commutative case is recovered [37, 39].

The behavior of the ratio proper time to coordinate time of Lyapunov exponent as a function of the circular orbits r_c in the NC spacetime is shown in Fig. 8. As we observe, the ratio $\hat{\lambda}_p/\hat{\lambda}_c$ is real in two region and it's separated with an imaginary one, as in the case of the proper time Lyapunov exponent.

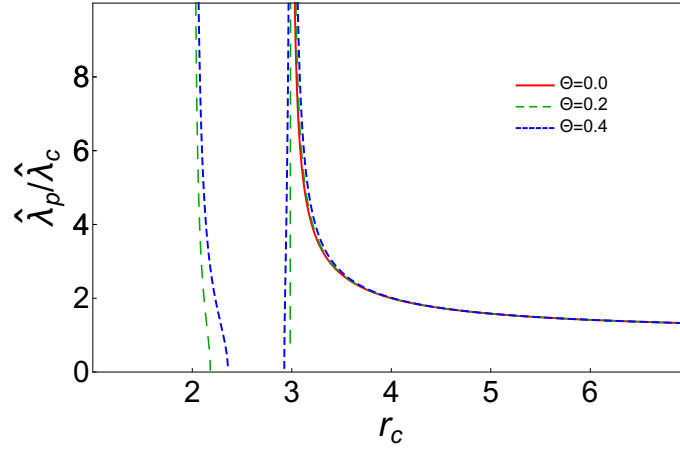


FIG. 8 The behavior of the ration proper time to coordinates time of Lyapunov exponent for a massive test particle in the NC Schwarzschild spacetime.

C. Radial motion of massless particles

In case of massless particle the radial motion in the NC SBH spacetime can be investigated using the effective potential (29) with $l = 0$ and $h = 0$, which gives us the radial motion

$$\left(\frac{dr}{d\tau}\right)^2 = E^2 - \Theta^2 \left\{ E^2 \left(\frac{m(64m^2 + m(-49 + 13\sqrt{1 - \frac{2m}{r}})r + 2(13 - 3\sqrt{1 - \frac{2m}{r}})r^2)}{16r^5(1 - \frac{2m}{r})^2} \right) \right\} + \mathcal{O}(\Theta^4) \quad (54)$$

the commutative expression is recovered when we set $\Theta = 0$. Now if we consider a photon in free fall into the NC SBH emitted from the point $r = r_0$ with $E = 1$, the affine parameter τ and coordinate time \hat{t} in this case is defined by

$$\hat{\tau} = - \int_{r_0}^r \left(1 - \Theta^2 \left\{ \left(\frac{m(64m^2 + m(-49 + 13\sqrt{1 - \frac{2m}{r}})r + 2(13 - 3\sqrt{1 - \frac{2m}{r}})r^2)}{16r^5(1 - \frac{2m}{r})^2} \right) \right\} \right)^{-1/2} dr, \quad (55)$$

$$\hat{t} = - \int_{r_0}^r (\hat{g}_{00})^{-1} \left(1 - \Theta^2 \left\{ \left(\frac{m(64m^2 + m(-49 + 13\sqrt{1 - \frac{2m}{r}})r + 2(13 - 3\sqrt{1 - \frac{2m}{r}})r^2)}{16r^5(1 - \frac{2m}{r})^2} \right) \right\} \right)^{-1/2} dr. \quad (56)$$

the integration of the both above equations are evaluated at the leading order in Θ , which give

$$\begin{aligned} \hat{\tau} = r_0 - r + \Theta \left\{ 25 \text{Log} \left(\frac{r_0(r - 2m)}{r(r_0 - 2m)} \right) - \frac{1}{128m} \left(\frac{32m^2 + 15mr_0 + 8r_0^2}{r_0^2} - \frac{32m^2 + 15mr + 8r^2}{r^2} \right) \right. \\ \left. + \frac{1}{128m} \left(\left(1 - \frac{2m}{r} \right)^{-1/2} - \left(1 - \frac{2m}{r_0} \right)^{-1/2} - 14 \left(\left(1 - \frac{2m}{r} \right)^{1/2} - \left(1 - \frac{2m}{r_0} \right)^{1/2} \right) \right. \right. \\ \left. \left. - \frac{13}{3} \left(\left(1 - \frac{2m}{r_0} \right)^{3/2} - \left(1 - \frac{2m}{r} \right)^{3/2} \right) - \frac{35}{2} \left(\frac{r_0(r - 2m) - r(r_0 - 2m)}{(r_0 - 2m)(r - 2m)} \right) \right) \right\}, \end{aligned} \quad (57)$$

$$\begin{aligned} \hat{t} = r_0 - r + 2m \text{Log} \left(\frac{r_0 - 2m}{r - 2m} \right) + \Theta^2 \left\{ - \frac{224m^2 - 201mr_0 + 63r_0^2}{128r_0(r_0 - 2m)^2} + \frac{224m^2 - 201mr + 63r^2}{128r_0(r - 2m)^2} \right. \\ \left. - \frac{(17m^2 - 24mr_0 + 8r_0^2)\sqrt{1 - \frac{2m}{r_0}}}{m(r_0 - 2m)^2} + \frac{(17m^2 - 24mr + 8r^2)\sqrt{1 - \frac{2m}{r}}}{m(r - 2m)^2} - \frac{63}{m} \text{Log} \left(\frac{r_0(r - 2m)}{r(r_0 - 2m)} \right) \right\}. \end{aligned} \quad (58)$$

the commutative affine parameter and coordinate time of massless particle are obtained when $\Theta = 0$ [5].

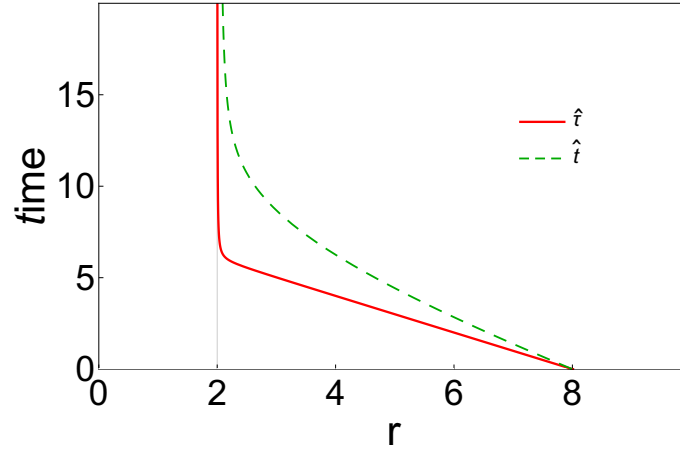


FIG. 9 The behavior of the affine parameter and the coordinate time along a radial null geodesic of a photon in the NC SBH as function of r .

The variation of the affine parameter \hat{t} and the coordinate time \hat{t} along a radial null geodesic is shown in Fig. 9. For a photon at $r = r_0$ falling toward the NC SBH, it is seen that for the case of the NC spacetime in the affine parameter framework, the photons take an infinite affine parameter to reach the NC singularity contrary to the commutative case [5, 72], and it's the same case for the time coordinate which takes an infinite time, which is the same behavior as in the commutative case for the time coordinate [5]. It is worth noting that, the non-commutativity prevents the photons from reaching the NC singularity only after an infinite affine parameter, which means the photons can not reach the singularity for a finite time, and that is the same observation as the massive particles.

D. Circular motion of massless particles and Lyapunov exponents

In which follows we focus on the null geodesic motion of photon around the NC SBH. The effective potential for the photon in this geometry is given by (29) with $h = 0$.

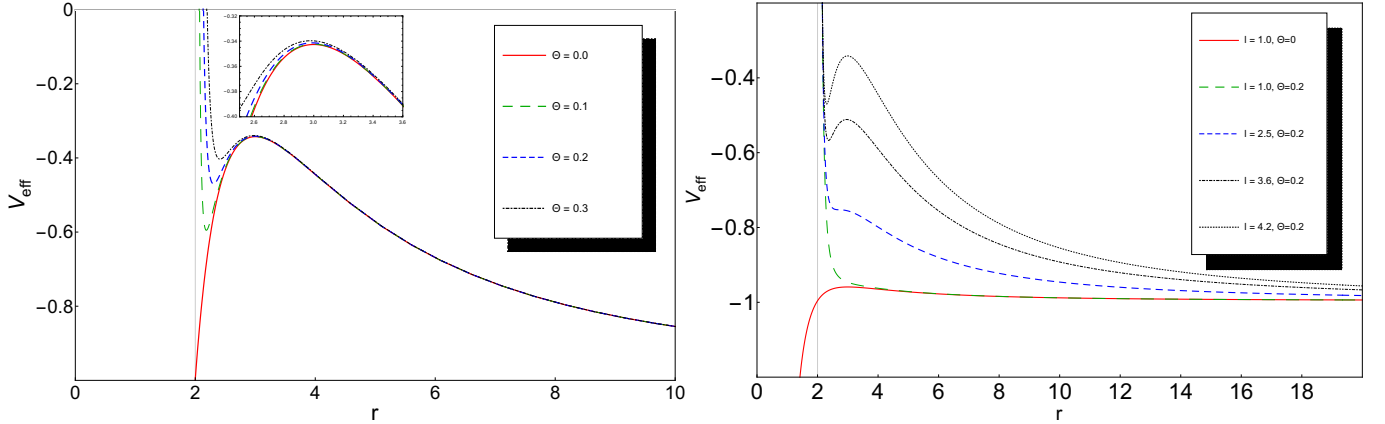


FIG. 10 The behavior of the effective potential for massless particle with different values of NC parameters Θ and fixed: $E = 0.998$, $m = 1$, $l = 4.2$ (left panel), and with different angular momentum l and fixed $E = 0.998$, $m = 1$, $\Theta = 0.2$ (right panel).

In Fig. 10 we show the influence of the NC parameters Θ (left panel) and the angular momentum l (right panel) on the effective potential for a massless particle (photon). As we observe now, there is a new minimum for the effective potential that appears near the event horizon in this geometry in a similar way as for the massive particle case, while for the massless one, there are only two extrema located outside the event horizon, and that allows us to interpret this new minimum as a new stable circular orbit, which gives a stable photon sphere in this geometry. It is worth to note that, the new minimum of the effective potential shifts away from the event horizon as Θ increases,

and the NC effects become insignificant as we move further from the event horizon ($r \gg r_h^{NC}$). In the right panel, it is clear that in the NC spacetime, there is a condition in angular momentum in which the effective potential has an extremum, contrary to the commutative case where the effective potential has a maximum, whatever the value of the angular momentum, in our case of $\Theta = 0.2$ this potential has always two extremum for critical angular momentum $l^{crit} \geq 2.55$, and these values depend on the NC parameter. As a conclusion, in the NC spacetime, there is always a two-photon sphere, where the inner one is stable and the outer is unstable.

1. Null circular orbit and photon sphere

The circular orbit of photon subjects to the same condition as the massive particle (36), using the effective potential (29) with $h = 0$, which leads to the ratio between the energy E_c and the angular momentum L_c by the following expression:

$$\frac{1}{D_c} = \frac{E_c}{L_c} = \sqrt{\frac{r_c - 2m}{r_c^3} + \left(\frac{J(r_c) + G(r_c) \sqrt{1 - \frac{2m}{r_c}}}{16r_c^6(r_c - 2m)} \right) \Theta^2}. \quad (59)$$

where D_c is the impact parameter, and

$$J(r_c) = 156m^3 - 185m^2r_c + 73mr_c^2 - 10r_c^3, \quad G(r_c) = 33m^2r_c - 37mr_c^2 + 6r_c^3. \quad (60)$$

TABLE I Some numerical values of unstable r_{uns} and new stable circular orbit r_{sta} of photon sphere in the NC spacetime with different parameter Θ and fixed $E = 0.998$, $l = 4.2$, $m = 1$.

Θ	0	0.10	0.15	0.20	0.25	0.30
$r_{sta}(new)$	2.18400	2.24624	2.30383	2.35865	2.41183	
r_{uns}	3.	2.99782	2.99504	2.99101	2.98559	2.97855

This table I shows some numerical solution of equation (36), which represents the variation of stable and unstable circular orbits of photon sphere as a function of Θ , where these two types of circular orbits get closer to each other as Θ increases, for $3.29 \leq l \leq 4.48$ (the condition on l depends on $0 \leq \Theta \leq 0.3$), where the stable circular orbit increasing and the unstable one decreasing, while for $l > 4.48$ these circular orbits increase both of them with increasing Θ .

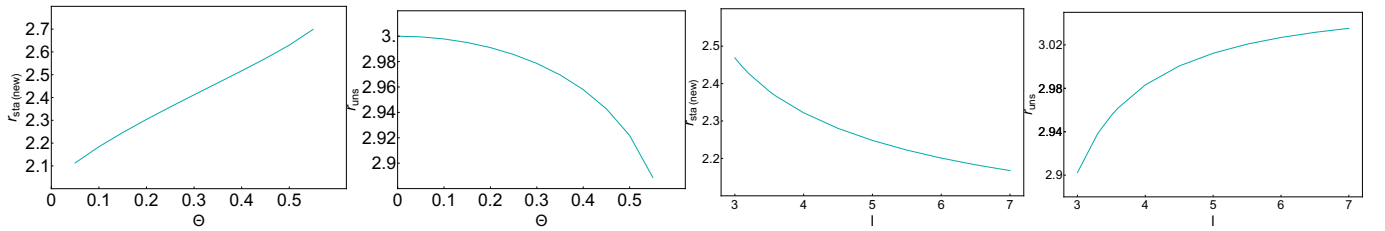


FIG. 11 The behavior of the photon sphere radius in the NC spacetime. stable and unstable circular orbit as function of Θ and for fixed $l = 4.2$, $E = 1$, $m = 1$ (two left panels), and as function of l and for fixed $\Theta = 0.3$, $E = 1$, $m = 1$ (two right panels).

As we see in Fig. 5 (two left panels) that as the NC parameter Θ increases, the new stable null circular orbit increases, while the unstable one decreases. Therefore the unstable circular orbital of the photon has a smaller radius in NC spaces as the parameter increases for the case $l < 4.48$ and is greater than the commutative case for $l \geq 4.48$, where this orbit in the commutative case is independent of the angular momentum l , and that is due to the modification in the gravitational field by the non-commutativity. For the two right panels Fig. 5, the new stable circular orbit decreases as the angular momentum l increases in this geometry, while the unstable one increases.

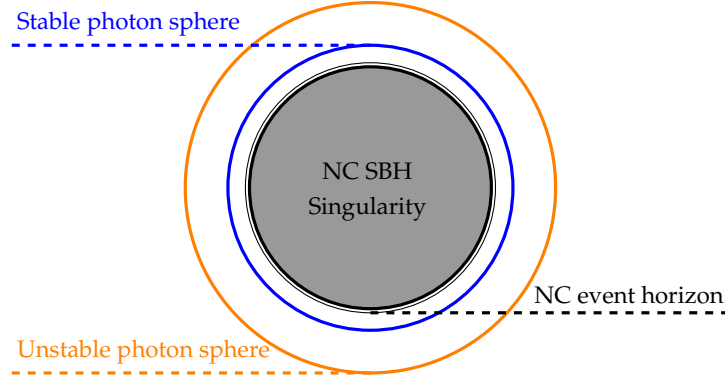


FIG. 12 The schematic picture of the stable/unstable photon sphere around the NC SBH.

2. Lyapunov exponents

As we know, for the null circular orbit of photons, there is no proper time, and that leaves us with only one Lyapunov exponent, which is the coordinate time.

Firstly we compute the angular frequency and the time period in coordinate time, which is given by (41) and (45) respectively,

$$\hat{\Omega}_c^{Null} = \frac{1}{D_c}, \quad \hat{T}_{\hat{\Omega}}^{Null} = 2\pi D_c \quad (61)$$

Now, we derive the coordinate time Lyapunov exponent for the photons orbit around NC SBH.

$$\hat{\lambda}_c^{Null} = \sqrt{-\frac{3((-4m + r_c)(-2m + r_c))}{r_c^4} + \left(\frac{O(r_c) + I(r_c)\sqrt{1 - \frac{2m}{r_c}}}{32(r_c - 2m)^2 r_c^7}\right)^2} \Theta^2. \quad (62)$$

where

$$O(r_c) = -19488m^5 + 39000m^4 r_c - 29076m^3 r_c^2 + 9958m^2 r_c^3 - 1716m r_c^4 + 140r_c^5, \quad (63)$$

$$I(r_c) = -3171m^4 r_c + 5773m^3 r_c^2 - 3908m^2 r_c^3 + 1080m r_c^4 - 84r_c^5. \quad (64)$$

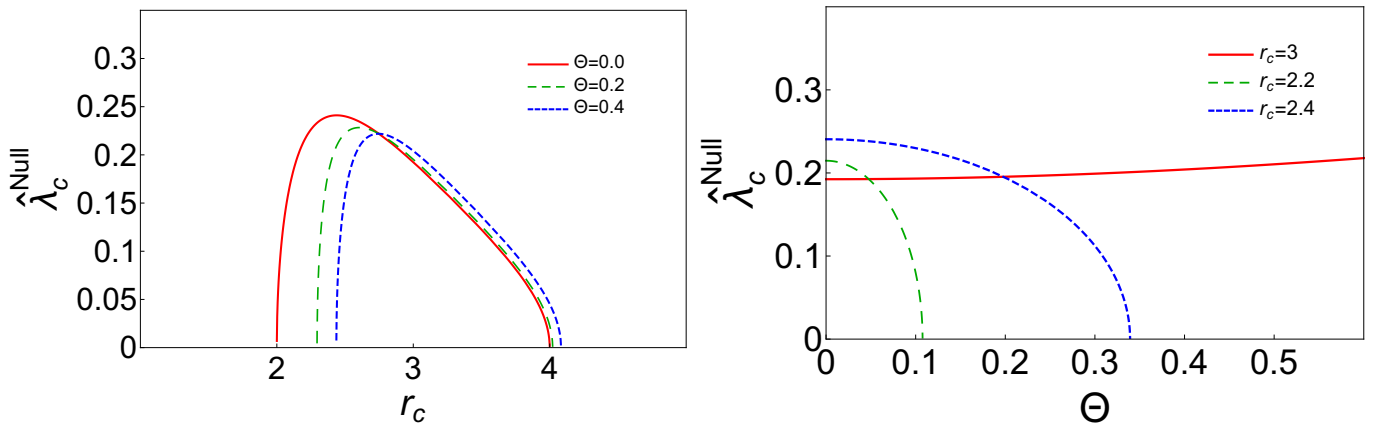


FIG. 13 The behavior of the coordinate time Lyapunov exponent for massless particle as a function of r_c (left panel), and as a function of the NC parameters Θ (right panel).

The Fig. 13, shows the behavior of the coordinate time Lyapunov exponent for photon as a function of r_c (left panel), and as a function of the NC parameters Θ (right panel). As we see in the left panel, the instability increases

rapidly to the maximum (where this maximum decreases as Θ increases.), then decreases as r_c increases until reaches zero for $r_c \geq 4$. It is worth noting that, in the NC case the instability of orbit is small compared to the commutative case for the orbit near the event horizon, and this observation is reflected when we move away from the event horizon. In the commutative case, the instability of the orbits begins from the event horizon, but in the NC spacetime this instability is shifted away from the event horizon which left some stable orbits near the event horizon and that is what we found in our previous discussion of the effective potential for a massless particle which correspond to the stable photon sphere of NC SBH, and that is the same observation in other theory of non-commutativity as in Ref. [65] where in this theory the orbit is located inside the event horizon, which can't be seen as stable photon sphere around NC SBH. Also, we check the instability of some orbits r_c as a function of the NC parameter Θ (right panel), it can be observed that the orbit $r_c = 3$ is also unstable in the NC spacetime where this geometry increases the instability of this orbit. For others, a new circular orbit near the event horizon that emerged in the NC spacetime has less instability and decreases as Θ increases before going to zero for specified values of Θ , and that indicates that some circular orbits near the event horizon in NC space-time are stable.

The instability exponent of null circular orbits in the NC spacetime is defined by the ratio of Lyapunov exponent to angular frequency in the coordinate time ($\hat{\lambda}_c^{Null} / \hat{\Omega}_c^{Null}$), which give us

$$\frac{\hat{\lambda}_c^{Null}}{\hat{\Omega}_c^{Null}} = \sqrt{\frac{3(4m - r_c)}{r_c} + \left(\frac{O(r_c) + 6J(r_c)(8m^2 - 6mr_c + r_c^2) + (I(r_c) + 6G(r_c)(8m^2 - 6mr_c + r_c^2))\sqrt{1 - \frac{2m}{r_c}}}{32(r_c - 2m)^3 r_c^4} \right) \sqrt{1 - \frac{2m}{r_c}}} \Theta^2. \quad (65)$$

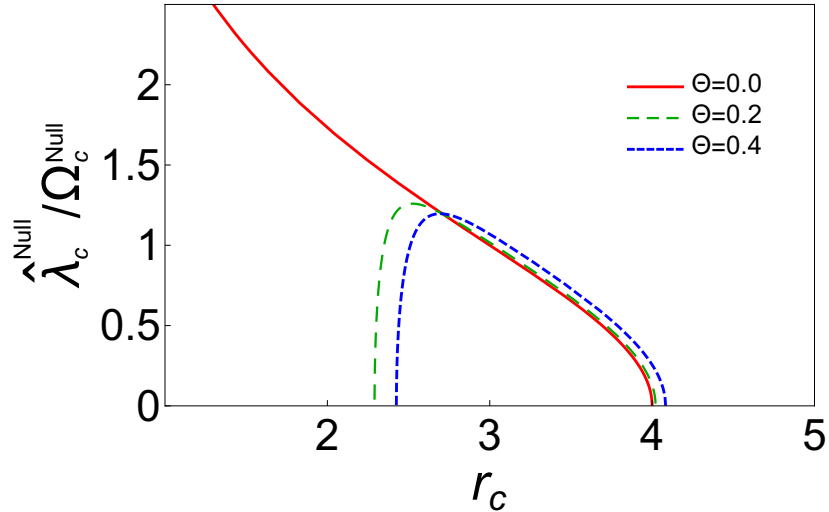


FIG. 14 The behavior of the ratio of Lyapunov exponent to angular frequency in the coordinate time as function of r_c .

The variation of the ratio $\hat{\lambda}_c^{Null} / \hat{\Omega}_c^{Null}$ as function of r_c is depicted in Fig. 14. As we see, this ratio shows the same behavior as in Fig. 13, except for the commutative case, which means that the orbits near the event horizon in the NC spacetime are stable contrary to the results obtained in Ref. [65].

As final analysis of instability we check the critical exponent $\hat{\gamma}$ for the null circular orbit around NC SBH, which is defined as a ratio of Lyapunov timescale $\hat{T}_{\hat{\lambda}} = \frac{2\pi}{\hat{\lambda}}$ to the orbital timescale $\hat{T}_{\hat{\Omega}} = \frac{2\pi}{\hat{\Omega}}$ [31–33], in this case we get:

$$\hat{\gamma}^{Null} = \frac{T_{\hat{\lambda}}^{Null}}{T_{\hat{\Omega}}^{Null}} = \frac{1}{2\pi \sqrt{\frac{3(4m - r_c)}{r_c} + \left(\frac{O(r_c) + 6J(r_c)(8m^2 - 6mr_c + r_c^2) + (I(r_c) + 6G(r_c)(8m^2 - 6mr_c + r_c^2))\sqrt{1 - \frac{2m}{r_c}}}{32(r_c - 2m)^3 r_c^4} \right) \sqrt{1 - \frac{2m}{r_c}}} \Theta^2}. \quad (66)$$

in limit of $\Theta = 0$ we recover the commutative expression.

The Table. II we show some numerical values of the critical exponent $\hat{\gamma}^{Null}$ for the photons, for different range of orbits r_c and different NC parameter Θ . As we can see from this table there are real and imaginary values, where the real positive values of this quantity $\hat{\gamma}^{Null}$ for the range of r_c correspond to unstable circular orbits [32], and the

TABLE II Some numerical values of the critical exponent $\hat{\gamma}^{Null}$ for unstable r_{uns} and new stable circular orbit r_{sta} of photon sphere in the NC spacetime with different parameter Θ with $m = 1$.

Θ	$r_c = 3$	$r_c = 2.4$	$r_c = 2.3$	$r_c = 2.2$
0.0	0.159155	//	//	//
0.1	0.158439	0.117291	0.121293	0.251639
$\hat{\gamma}^{Null}$ 0.2	0.156349	0.136225	0.328429	0. -0.0662942 i
0.3	0.153042	0.210585	0. -0.10626 i	0. -0.0397438 i
0.4	0.148746	0. -0.216564 i	0. -0.0665877 i	0. -0.0288573 i

imaginary ones correspond to the stable one. It is worth noting that the ordinary orbit of the photon sphere around SBH $r_c = 3$ is always unstable, also in the NC spacetime according to the definition (66) means that the Lyapunov timescale is shorter than the orbital timescale ($\hat{T}_{\lambda} < \hat{T}_{\Omega}$) [31] and the same observation for all real values of $\hat{\lambda}^{Null}$ for the others ranges of r_c in this table. Also, we show the effect of the NC parameter in the values of $\hat{\lambda}^{Null}$, where these values are decreasing with the increase of Θ for $r_c = 3$, and the smallest one of $\hat{\lambda}^{Null}$ indicates a strong Lyapunov instability [33] (see right panel Fig. 13), while the imaginary values which correspond to the stable circular orbit coincide with the new minimum location of the effective potential for $l = 5.2$ (close values to the values of Table. I), and that shows the stability of the new stable photon sphere around NC SBH and prove the instability of the external photon sphere in both of commutative and non commutative spacetime.

3. Black hole shadow

In the equatorial plane $\theta = \pi/2$, it is easy to show that, the radius of the black hole shadow R_{shadow} is related to the impact parameter D_c by the relation $R_{shadow} = D_c|_{r=r_{ps}}$, where r_{ps}^{uns} is the radius of the unstable photon sphere, which can be obtained by solving $\frac{dV_{eff}}{dr} = 0$, and the solution to this equation in the leading order in Θ and m is given by:

$$r_{ps}^{uns} = 3m - \left(\frac{-38 + 540D_c^2 m^2}{288m} \right) \Theta^2. \quad (67)$$

It is worth to note that, the new stable photon sphere is only obtained by numerical solution (see Tab. II). Using this expression, we can express the radius of the NC SBH shadow

$$R_{shadow} = 3\sqrt{3}m \left(1 + \frac{(1 + 2\sqrt{3})}{72m^2} \Theta^2 \right). \quad (68)$$

where the commutative expression can be obtained by setting $\Theta = 0$.

Fig. 15 shows the NC SBH shadow for different values of Θ (left panel) and m (right panel). As we see in the left panel, the shadow radius of NC SBH increases with the increasing Θ , and it's the same note in the right panel for the fixed NC parameter and increasing in the black hole mass m . Moreover, we can see a similar effect of the non-commutativity and the black hole mass on the shadow radius, where the NC property of spacetime plays a similar role as a mass, and that's what was expected in our previous work [62], and that means to increase the gravitational field. It is worth to motioned that, this observation it's the same one obtained in [73], in which the authors used the NC correction to the black hole mass using gauge theory of gravity with negligence of the metric correction. However, in our case, we use the NC Schwarzschild metric to describe the radius of the NC SBH shadow.

4. Energy emission rate

In order to investigate the unstable photon sphere emission in the NC spacetime, we compute the energy emission rate [74, 75], and it's given by:

$$\frac{d^2 \hat{E}}{d\omega dt} = \frac{2\pi^2 \hat{\sigma}_{lim} \omega^3}{e^{\omega/\hat{T}} - 1}, \quad (69)$$

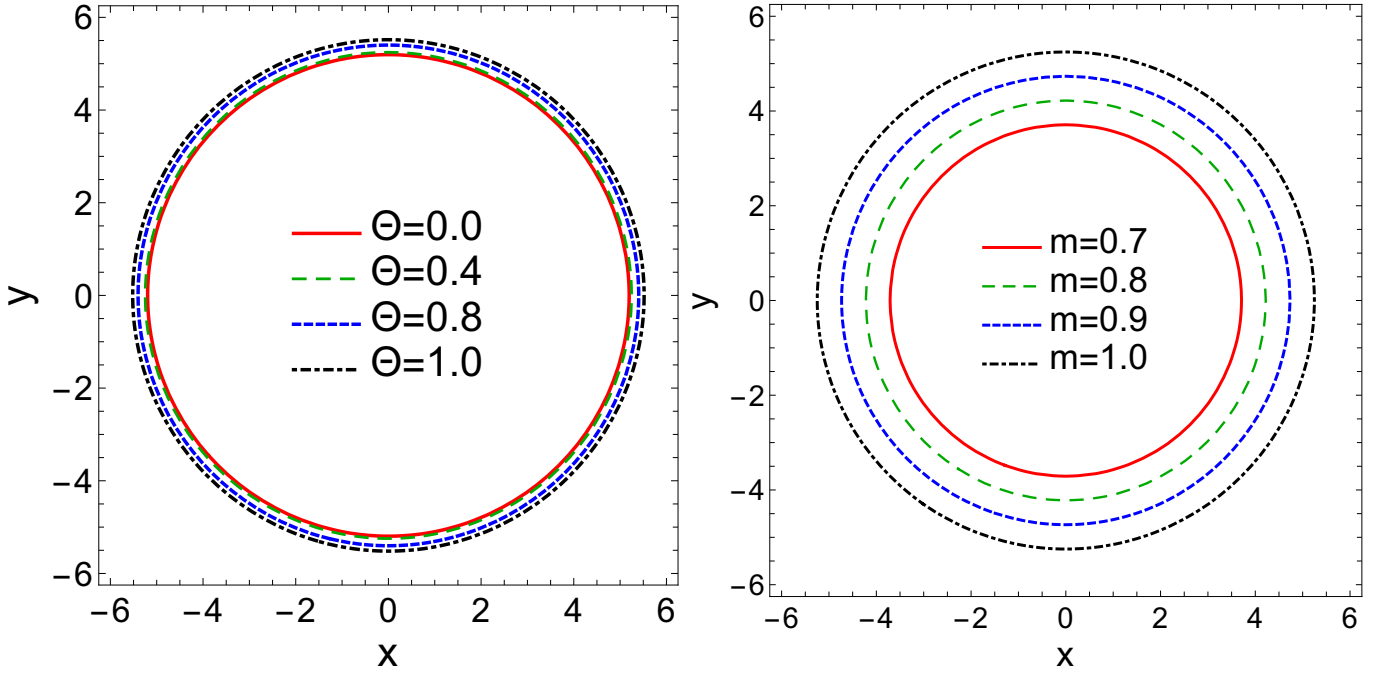


FIG. 15 The SBH shadow in the NC spacetime, for different values of NC parameter Θ (left panel) with $m = 1$, and for different values of black hole mass m (right panel) with $\Theta = 0.4$.

where deformed Hawking temperature of this black hole is given by $\hat{T} = \frac{1}{4\pi r_h} \left(1 - \frac{\Theta^2}{r_h^2}\right)$ (for more detail see Ref. [70]), $\hat{\sigma}$ denoted the frequency of emitted particles, and σ_{lim} is the greybody factor, which is appreciatively related to the radius of black hole shadow by $\hat{\sigma}_{lim} = \pi R_{shadow}^2$. By substituting this relation into the above equation, we find

$$\frac{d^2 \hat{E}}{d\omega dt} = \frac{2\pi^3 R_{shadow}^2 \omega^3}{e^{\omega/\hat{T}} - 1}, \quad (70)$$

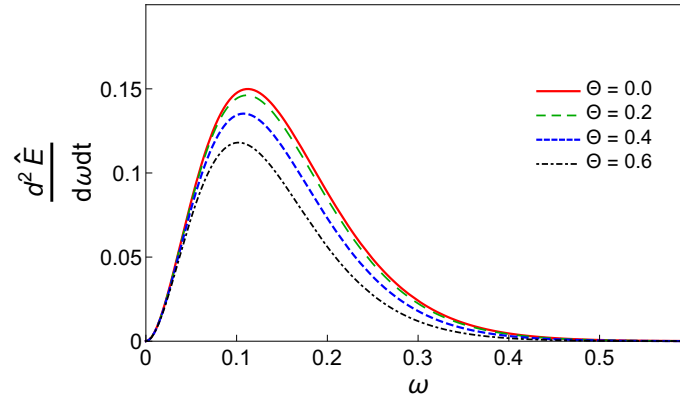


FIG. 16 Behavior of the NC energy emission rate of SBH as a function of frequency ω .

In Fig. 16, we illustrate the behavior of NC energy emission rate of SBH as a function of the frequency ω and for different NC parameter Θ . As we observe, there is a gaussian distribution peak of energy emission rate also in the NC spacetime. It is clear that, this geometry decreases the peak and shifts it toward the low frequency with Θ increase.

IV. CONCLUSIONS

In this paper, we study the geodesic motion for both massive and massless particles in NC Schwarzschild space-time. The background used for our calculation is the deformed SBH via the SW maps and the star product in the context of the gauge theory of gravity [62], where the deformed metric was obtained in the leading order in Θ , according to the deformed metric we obtain the correction to the effective potential up to the second order in Θ .

As a first step, we investigate the radial motion for both massive particles and massless ones, where we compute the correction to the affine parameter and coordinate time in this geometry. Our results show that the massive and massless particles take an infinite time to reach the NC singularity and NC event horizon in both of affine parameter framework and coordinate time respectively, where that's the effect of the non-commutativity which prevents particles from reaching the NC singularity at a finite proper time (affine parameter for photons).

Moreover, we examine the geodesic stability using the Lyapunov exponent to establish the instability of circular orbits for both massive and massless particles. In the case of massive particles, we compute the angular frequency $\hat{\Omega}_c$ and the period time \hat{T}_c in NC spacetime, and we describe both of the proper time Lyapunov exponent $\hat{\lambda}_p$ and the coordinate time one $\hat{\lambda}_c$ in this geometry, where the proper time one shows a new behavior which allows the existence of a stable region between two unstable ones near the event horizon, and this agrees with our results in previous work [62], and the same observation for their ratio. For the massless particles case, we study the effective potential of this type of particles, we show a new kind of motion near the event horizon, which is interpreted as a new stable circular orbit in the NC spacetime, and that is a new photon sphere near the event horizon that is stable compared to the commutative one. In this geometry, the NC SBH has two-photon spheres, and the first one can be seen as the inner photon sphere which is considered stable while the outer one is unstable. Then the coordinate time Lyapunov exponent $\hat{\lambda}_c^{Null}$ is expressed to describe the instability of the photon sphere, where our results show that the outer photon sphere is unstable in both commutative and NC spacetime, while for the inner photon sphere is stable and only allowed in the NC spacetime. Also the critical exponent $\hat{\gamma}^{Null}$ is computed to analyze the instability of the null circular orbit around the NC SBH. It is worth noting that, the all commutative expression in this paper can be recovered when we put $\Theta = 0$. Finally, we show the effect of the non-commutativity on the shadow of SBH, and show a similarity between the mass and the non-commutativity based on our results, which indicates that the NC propriety of spacetime increases the gravitational field of the SBH. Then show the effect of this geometry on the energy emission rate of SBH, where the non-commutativity decrease this energy, and that agree with our remark for the effect on SBH shadow. However, more studies of this phenomenon may help to understand more about this geometry and its effect on the black hole theory.

Acknowledgments

This work is supported by project B00L02UN050120230003, Univ. Batna 1, Algeria.

-
- [1] A. Eckart, R. Genzel, T. Ott, and R. Schödel. Stellar orbits near sagittarius a*. *Monthly Notices of the Royal Astronomical Society*, 331(4):917–934, 04 2002.
 - [2] S Gillessen, Frank Eisenhauer, TK Fritz, H Bartko, K Dodds-Eden, O Pfuhl, T Ott, and R Genzel. The orbit of the star s2 around sgr a* from very large telescope and keck data. *The Astrophysical Journal*, 707(2):L114, 2009.
 - [3] RI Gainutdinov. Ppn motion of s-stars around sgr a*. *Astrophysics*, 63(4):470–481, 2020.
 - [4] Florian Peißker, Andreas Eckart, Michal Zajaček, Basel Ali, and Marzieh Parsa. S62 and s4711: Indications of a population of faint fast-moving stars inside the s2 orbit—s4711 on a 7.6 yr orbit around sgr a*. *The Astrophysical Journal*, 899(1):50, 2020.
 - [5] Chandrasekhar Subrahmanyan. *Mathematical Theory of Black Holes*. Oxford University Press, 1999.
 - [6] GW Gibbons, CM Warnick, and MC Werner. Light bending in schwarzschild–de sitter: projective geometry of the optical metric. *Classical and Quantum Gravity*, 25(24):245009, 2008.
 - [7] JN Islam. The cosmological constant and classical tests of general relativity. *Physics Letters A*, 97(6):239–241, 1983.
 - [8] MJ Jaklitsch, Charles Hellaby, and DR Matravers. Particle motion in the spherically symmetric vacuum solution with positive cosmological constant. *General relativity and gravitation*, 21(9):941–951, 1989.
 - [9] Zdenek Stuchlik and Massimo Calvani. Null geodesics in black hole metrics with non-zero cosmological constant. *General Relativity and Gravitation*, 23(5):507–519, 1991.
 - [10] GV Kraniotis and SB Whitehouse. Compact calculation of the perihelion precession of mercury in general relativity, the cosmological constant and jacobi's inversion problem. *Classical and Quantum Gravity*, 20(22):4817, 2003.
 - [11] GV Kraniotis. Precise relativistic orbits in kerr–(anti) de sitter spacetimes. *Classical and Quantum Gravity*, 21(19):4743, 2004.

- [12] Norman Cruz, Marco Olivares, and Jose R Villanueva. The geodesic structure of the schwarzschild anti-de sitter black hole. *Classical and Quantum Gravity*, 22(6):1167, 2005.
- [13] Eva Hackmann, Valeria Kagramanova, Jutta Kunz, and Claus Lämmerzahl. Analytic solutions of the geodesic equation in higher dimensional static spherically symmetric spacetimes. *Physical Review D*, 78(12):124018, 2008.
- [14] Valeria Kagramanova, Jutta Kunz, Eva Hackmann, and Claus Lämmerzahl. Analytic treatment of complete and incomplete geodesics in taub-nut space-times. *Physical Review D*, 81(12):124044, 2010.
- [15] Eva Hackmann, Claus Lämmerzahl, Valeria Kagramanova, and Jutta Kunz. Analytical solution of the geodesic equation in kerr-(anti-) de sitter space-times. *Physical Review D*, 81(4):044020, 2010.
- [16] Eva Hackmann, V Kagramanova, J Kunz, and C Lämmerzahl. Analytic solutions of the geodesic equation in axially symmetric space-times. *EPL (Europhysics Letters)*, 88(3):30008, 2009.
- [17] Janna Levin and Gabe Perez-Giz. A periodic table for black hole orbits. *Physical Review D*, 77(10):103005, 2008.
- [18] Saskia Grunau and Valeria Kagramanova. Geodesics of electrically and magnetically charged test particles in the reissner-nordström space-time: analytical solutions. *Physical Review D*, 83(4):044009, 2011.
- [19] Edward Belbruno and Frans Pretorius. A dynamical system’s approach to schwarzschild null geodesics. *Classical and Quantum Gravity*, 28(19):195007, 2011.
- [20] Leor Barack and Norichika Sago. Beyond the geodesic approximation: Conservative effects of the gravitational self-force in eccentric orbits around a schwarzschild black hole. *Physical Review D*, 83(8):084023, 2011.
- [21] Daniela Pugliese, Hernando Quevedo, and Remo Ruffini. Circular motion of neutral test particles in reissner-nordström spacetime. *Physical Review D*, 83(2):024021, 2011.
- [22] Daniela Pugliese, Hernando Quevedo, and Remo Ruffini. Circular motion in reissner–nordström spacetime. In *The Twelfth Marcel Grossmann Meeting: On Recent Developments in Theoretical and Experimental General Relativity, Astrophysics and Relativistic Field Theories (In 3 Volumes)*, pages 1017–1021. World Scientific, 2012.
- [23] Kumar S Virbhadra and George FR Ellis. Gravitational lensing by naked singularities. *Physical Review D*, 65(10):103004, 2002.
- [24] KS Virbhadra and CR Keeton. Time delay and magnification centroid due to gravitational lensing by black holes and naked singularities. *Physical Review D*, 77(12):124014, 2008.
- [25] Parthapratim Pradhan and Parthasarathi Majumdar. Circular orbits in extremal reissner–nordstrom spacetime. *Physics Letters A*, 375(3):474–479, 2011.
- [26] Marco Olivares, Joel Saavedra, Carlos Leiva, and Jose R Villanueva. Motion of charged particles on the reissner–nordström (anti-)de sitter black hole spacetime. *Modern Physics Letters A*, 26(39):2923–2950, 2011.
- [27] JR Villanueva, Joel Saavedra, Marco Olivares, and Norman Cruz. Photons motion in charged anti-de sitter black holes. *Astrophysics and Space Science*, 344(2):437–446, 2013.
- [28] Daniela Pugliese, Hernando Quevedo, and Remo Ruffini. Motion of charged test particles in reissner-nordström spacetime. *Physical Review D*, 83(10):104052, 2011.
- [29] Daniela Pugliese, Hernando Quevedo, and Remo Ruffini. General classification of charged test particle circular orbits in reissner–nordström spacetime. *The European Physical Journal C*, 77(4):1–18, 2017.
- [30] Aleksandr Mikhailovich Lyapunov. The general problem of the stability of motion. *International journal of control*, 55(3):531–534, 1992.
- [31] Neil J Cornish and Janna Levin. Lyapunov timescales and black hole binaries. *Classical and Quantum Gravity*, 20(9):1649, 2003.
- [32] Frans Pretorius and Deepak Khurana. Black hole mergers and unstable circular orbits. *Classical and Quantum Gravity*, 24(12):S83, 2007.
- [33] Vitor Cardoso, Alex S Miranda, Emanuele Berti, Helvi Witek, and Vilson T Zanchin. Geodesic stability, lyapunov exponents, and quasinormal modes. *Physical Review D*, 79(6):064016, 2009.
- [34] MR Setare and D Momeni. Geodesic stability for kehagias-sfetsos black hole in hořava-lifshitz gravity via lyapunov exponents. *International Journal of Theoretical Physics*, 50:106–113, 2011.
- [35] Sharmanthie Fernando. Schwarzschild black hole surrounded by quintessence: null geodesics. *General Relativity and Gravitation*, 44:1857–1879, 2012.
- [36] B Malakolkalami and K Ghaderi. Schwarzschild-anti de sitter black hole with quintessence. *Astrophysics and Space Science*, 357(2):112, 2015.
- [37] Parthapratim Pradhan. Stability analysis and quasinormal modes of reissner–nordström space-time via lyapunov exponent. *Pramana*, 87:1–9, 2016.
- [38] K Ghaderi. Geodesics of black holes with dark energy. *Astrophysics and Space Science*, 362(12):218, 2017.
- [39] Monimala Mondal, Parthapratim Pradhan, Farook Rahaman, and Indrani Karar. Geodesic stability and quasi normal modes via lyapunov exponent for hayward black hole. *Modern Physics Letters A*, 35(30):2050249, 2020.
- [40] Shobhit Giri and Hemwati Nandan. Stability analysis of geodesics and quasinormal modes of a dual stringy black hole via lyapunov exponents. *General Relativity and Gravitation*, 53(8):76, 2021.
- [41] Monimala Mondal, Farook Rahaman, and Ksh Newton Singh. Lyapunov exponent, isco and kolmogorov–senai entropy for kerr–kiselev black hole. *The European Physical Journal C*, 81:1–16, 2021.
- [42] Stephen W Hawking. Particle creation by black holes. In *Euclidean quantum gravity*, pages 167–188. World Scientific, 1975.
- [43] G. W. Gibbons and S. W. Hawking. Action integrals and partition functions in quantum gravity. *Phys. Rev. D*, 15:2752–2756, May 1977.
- [44] Shahar Hod. Bohr’s correspondence principle and the area spectrum of quantum black holes. *Physical Review Letters*, 81(20):4293, 1998.
- [45] Cenalo Vaz. Canonical quantization and the statistical entropy of the schwarzschild black hole. *Physical Review D*,

- 61(6):064017, 2000.
- [46] B Harms and Y Leblanc. Statistical mechanics of black holes. *Physical Review D*, 46(6):2334, 1992.
 - [47] Gilad Gour. Schwarzschild black hole as a grand canonical ensemble. *Physical Review D*, 61(2):021501, 1999.
 - [48] Slimane Zaim and Hadjar Rezki. Thermodynamic properties of a yukawa–schwarzschild black hole in noncommutative gauge gravity. *Gravitation and Cosmology*, 26(3):200–207, 2020.
 - [49] N Mebarki, S Zaim, L Khodja, and H Aisaoui. Gauge gravity in noncommutative de sitter space and pair creation. *Physica Scripta*, 78(4):045101, 2008.
 - [50] KOUROSH NOZARI and BEHNAZ FAZLPUR. Thermodynamics of noncommutative schwarzschild black hole. *Modern Physics Letters A*, 22(38):2917–2930, 2007.
 - [51] Kourosh Nozari and Behnaz Fazlpour. Reissner-nordström black hole thermodynamics in noncommutative spaces, 2006.
 - [52] Ravi Shankar Kuniyal, Rashmi Uniyal, Anindya Biswas, Hemwati Nandan, and KD Purohit. Null geodesics and red–blue shifts of photons emitted from geodesic particles around a noncommutative black hole space–time. *International Journal of Modern Physics A*, 33(16):1850098, 2018.
 - [53] B Mirza and M Dehghani. Noncommutative geometry and classical orbits of particles in a central force potential. *Communications in Theoretical Physics*, 42(2):183, 2004.
 - [54] Juan M Romero and J David Vergara. The kepler problem and noncommutativity. *Modern Physics Letters A*, 18(24):1673–1680, 2003.
 - [55] Sehrish Iftikhar. Particle dynamics around a charged black hole. In *EPJ Web of Conferences*, volume 168, page 04006. EDP Sciences, 2018.
 - [56] SC Ulhoa, RGG Amorim, and AF Santos. On non-commutative geodesic motion. *General Relativity and Gravitation*, 46(7):1760, 2014.
 - [57] Alexis Larranaga. Geodesic structure of the noncommutative schwarzschild anti-de sitter black hole i: timelike geodesics. *arXiv preprint arXiv:1110.0778*, 2011.
 - [58] Kourosh Nozari, Siamak Akhshabi, and Nasser Sadeghnezhad. Stability of circular orbits in noncommutative schwarzschild spacetime. *Acta Physica Polonica B*, 39(11), 2008.
 - [59] Piero Nicolini. Noncommutative black holes, the final appeal to quantum gravity: a review. *International Journal of Modern Physics A*, 24(07):1229–1308, 2009.
 - [60] Piyali Bhar, Farook Rahaman, Ritabrata Biswas, and UF Mondal. Particles and scalar waves in noncommutative charged black hole spacetime. *Communications in Theoretical Physics*, 64(1):1, 2015.
 - [61] F Rahaman, I Radinschi, UF Mondal, and P Bhar. Particle’s motion around a non-commutative black hole. *International Journal of Theoretical Physics*, 54(3):1038–1051, 2015.
 - [62] Abdellah Touati and Slimane Zaim. Geodesic equation in non-commutative gauge theory of gravity. *Chinese Physics C*, 46(10):105101, jun 2022.
 - [63] Grigoris Panotopoulos and Ángel Rincón. Quasinormal modes of five-dimensional black holes in non-commutative geometry. *The European Physical Journal Plus*, 135(1):33, 2020.
 - [64] Avijit Bera, Surojit Dalui, Subir Ghosh, and Elias C Vagenas. Quantum corrections enhance chaos: Study of particle motion near a generalized schwarzschild black hole. *Physics Letters B*, 829:137033, 2022.
 - [65] Shobhit Giri, Hemwati Nandan, Lokesh Kumar Joshi, and Sunil D Maharaj. Geodesic stability and quasinormal modes of non-commutative schwarzschild black hole employing lyapunov exponent. *The European Physical Journal Plus*, 137(2):1–11, 2022.
 - [66] Nathan Seiberg and Edward Witten. String theory and noncommutative geometry. *Journal of High Energy Physics*, 1999(09):032, 1999.
 - [67] Xavier Calmet and Archil Kobakhidze. Second order noncommutative corrections to gravity. *Physical Review D*, 74(4):047702, 2006.
 - [68] Paolo Aschieri and Leonardo Castellani. Noncommutative $d=4$ gravity coupled to fermions. *Journal of High Energy Physics*, 2009(06):086, 2009.
 - [69] Paolo Aschieri and Leonardo Castellani. Noncommutative gravity coupled to fermions: second order expansion via seiberg-witten map. *Journal of High Energy Physics*, 2012(7):1–27, 2012.
 - [70] Abdellah Touati and Slimane Zaim. Thermodynamic properties of schwarzschild black hole in non-commutative gauge theory of gravity. *Annals of Physics*, 455:169394, 2023.
 - [71] Ali H Chamseddine. Deforming einstein’s gravity. *Physics Letters B*, 504(1-2):33–37, 2001.
 - [72] Mohaddese Heydari-Fard, Malihe Heydari-Fard, and Hamid Reza Sepangi. Null geodesics and shadow of hairy black holes in einstein-maxwell-dilaton gravity. *Physical Review D*, 105(12):124009, 2022.
 - [73] N Heidari, H Hassanabadi, J Kuriuz, S Zare, PJ Porfirio, et al. Gravitational signatures of a non-commutative stable black hole. *arXiv preprint arXiv:2305.06838*, 2023.
 - [74] Shao-Wen Wei and Yu-Xiao Liu. Observing the shadow of einstein-maxwell-dilaton-axion black hole. *Journal of Cosmology and Astroparticle Physics*, 2013(11):063, 2013.
 - [75] A Belhaj, M Benali, A El Balali, H El Mounni, and SE Ennadifi. Deflection angle and shadow behaviors of quintessential black holes in arbitrary dimensions. *Classical and Quantum Gravity*, 37(21):215004, 2020.